DENTAL MATERIALS 35 (2019) 713–729

Available online at www.sciencedirect.com

ScienceDirect

journal homepage: www.intl.elsevierhealth.com/journals/dema

Properties of hot-pressed lithium silicate glass-ceramics

Lubica Hallmann[a], *Peter Ulmer*[b], *Mark-Daniel Gerngross*[c], *Justin Jetter*[c], *Michaël Mintrone*[b], *Frank Lehmann*[a,*], *Matthias Kern*[a]

[a] *Department of Prosthodontics, Propaedeutic and Dental Materials, School of Dentistry, Kiel University, Germany*
[b] *Institute of Geochemistry and Petrology, ETH Zürich, Switzerland*
[c] *Institute of Material Science, Faculty of Engineering, Kiel University, Germany*

ARTICLE INFO

Article history:
Received 19 December 2018
Accepted 13 February 2019

Keywords:
Hot-pressed LS2 glass-ceramics
Microstructure
Morphology of crystals
Fracture toughness
Biaxial flexural strength
Opacity
Color
Roughness
Chemical composition

ABSTRACT

Objectives. New lithium silicate/disilicate hot-pressed glass-ceramics are introduced into the dental market. It is known that the mechanical properties of this material depend on the microstructure, chemical composition, glass matrix, morphology of crystals, volume ratio crystal/glass, additive, and treatments. This contribution investigates how these factors affect the properties of the new generation of lithium silicate/disilicate hot-pressed glass-ceramics.

Methods. Three lithium silicate/disilicate hot-pressed glass-ceramics were investigated; IPS e.max Press (control group), Initial LiSi Press and Celtra Press. The specimens were prepared according to the manufacturers'instructions. Different methods; DTA, XRD, Raman, optical spectroscopy, SEM were used to characterize the properties of these materials before, after heat and etching treatments. The heat treatments (four firings) were performed according to the manufacturer's instructions (GC company) for veneering (initial LiSi) of LS2 glass-ceramics. The etching was performed according to the manufacturer's instruction. Vita ceramics etch gel (HF 5%) was used as an etching agent. The mechanical properties were investigated according to DIN EN ISO 6872:2015 and ASTM C 1327-08 instructions.

Results. DTA and XRD analysis revealed that the transformation of the lithium silicate (LS) phase to the LS2 phase was completed for IPS e.max and Initial LiSi Press ingots while for Celtra Press ingots it was not. After pressing, the rod-shaped crystals were aligned parallel to the extrusion direction, while the platelet-shaped crystals having an interlocking microstructure were not. The mechanical properties depend on the microstructure, the chemical composition, the crystals morphology, the volume crystal/glass ratio, and the treatments (heat and etching). ZrO_2 did not improved the mechanical properties. Etching with HF gel decreased the flexural strength. After four heat treatments, the biaxial flexural strength, the K_{IC}, the roughness and the optical properties were affected. According to the HT-XRD, IPS e.max Press ingots can be hot pressed up to 900 °C, the initial LiSi Press ingots up to 940 °C and Celtra Press ingots up to 880 °C.

* *Corresponding author at*: Department of Prosthodontics, Propaedeutics and Dental Materials, School of Dentistry, Kiel University, Arnold-Heller-Str.16, D-24105 Kiel, Germany.
E-mail address: lhallmann@proth.uni-kiel.de (F. Lehmann).
https://doi.org/10.1016/j.dental.2019.02.027

Significance. The properties of LS2 glass-ceramics depend on the chemical composition, the microstructure, the morphology of the crystals, the properties of the residual glass matrix, the volume ratio of crystal/glass, and the treatments (heat and etching).

1. Introduction

Concerns about metallic hypersensitivity, biocompatibility and aesthetics have driven the development of dental ceramic materials. The substitution of metallic substructures in dental applications is increasing. Ceramic materials have many advantages over metals, like aesthetics, lower thermal conductivity, chemical and abrasion resistance. They have light-transmitting and light-diffracting properties, are absolutely colour stable and enable an invisible transition of the restoration margin into dental tissues [1–8].

Flexural strength is a significant mechanical property to evaluate the strength of brittle materials [9–12]. Hardness of ceramic materials is also a significant property of these materials because it represents the resistance to permanent surface indentation or penetration [10,13]. Fracture toughness is another important property and is used to characterize the fracture resistance of brittle materials [14]. The critical stress intensity factor (K_{IC}) is used to measure the toughness of the materials expressing the resistance to crack propagation. It is used as an indicator for choosing the most suitable materials for specific applications [13–20]. All-ceramic restorations have been very popular in the last decades because of the applications of modern dental technologies and the improvement in the mechanical, aesthetic and biocompatible properties of these materials [5,6,21–24]. The development of dental ceramics with high flexural strength, high fracture toughness, high aesthetic and high chemical resistance is a formidable challenge in dental industry. The application of lithium disilicate glass-ceramics and yttria-stabilized tetragonal zirconia polycrystals in dental practise has significantly increased the popularity of all-ceramic restorations [1,5,6,23–30].

The hot-pressing technique based on the viscous flow of glass-ceramics has found a wide application in dental restoration because of net-shape processing, decreased porosity, increased Weibull modulus, increased flexural strength, excellent marginal fit [31–37]. Differences in mechanical properties for materials with similar chemical compositions are primarily due to their microstructure. The orientation of crystallites, their grain-size distribution and shape, the ratio of glass matrix to crystalline phase, and homogeneity dictate the flexural strength and fracture toughness of glass-ceramics [16,34].

Lithium disilicate glass-ceramics are extensively employed in restorative dentistry because of their superior aesthetic properties and their hardness being similar to that of natural teeth [37]. Because of its high strength and toughness, restorations produced with this material can be cemented by various techniques [5,26]. The structure of monolithic lithium disilicate can resist masticatory stress, dissipating it throughout the entire restoration [9]. The mechanical properties of lithium disilicate glass-ceramics depend on several factors: thermal history, additives, pressure and time (for hot-pressed), amount of nucleating agent, crystal morphology, microstructure, glass matrix, volume ratio crystal/glass, phase composition and chemical composition. The effect of different factors on the mechanical properties of lithium disilicate glass-ceramic has been in the focus of many researchers [34].

The present study focused on the properties of three dental hot-pressed lithium silicate/disilicate glass-ceramics; IPS e.max Press, Initial LiSi Press, and Celtra Press.

The aim of this investigation was to study the properties of these glass-ceramics and the effect of the heat and etching treatments on their properties.

2. Materials and methods

2.1. *Specimen preparation*

Three hot-pressed lithium silicate/disilicate glass-ceramics were used in this study: IPS e.max Press, Initial LiSi Press and Celtra Press (Table 1).

The wax method was used for the preparation of specimens according to the manufacturers'instructions. A Dekema 264i furnace was used for the preparation of the Initial LiSi Press specimens and an Ivoclar 3010 furnace for the preparation of the IPS e.max Press and Celtra Press specimens. The disc-shaped ($d = 14 \pm 2$ mm, and $h = 1.2 \pm 0.2$ mm) specimens were polished with SiC paper up to 4000 grits in water. For biaxial fractural strength and optical properties, specimens were prepared according to DIN EN ISO 6872:2015 ($n = 40$ of each). For SEM ($n = 6$), Vickers hardness and roughness ($n = 10$), XRD ($n = 6$), and Raman ($n = 6$) measurements specimens were additionally polished up to 1 μm diamond suspension. To investigate the effect of heat treatments on the properties of the glass-ceramics, the specimens were heat treated according to the firing schedule of Initial LiSi veneering ceramic (Table 2, GC company). To investigate the properties of the ingots, the disc specimens ($n = 42$, $h = 2$ mm) were prepared by cutting the ingots under copious water. After that, specimens were polished up to 1 μm diamond suspension.

To study the effect of etching on the flexural strength, the specimens were etched with 5% hydrofluoric etching gel (Vita Zahfabrik, Germany) according to the manufacturers' instructions (20 s).

2.2. *Differential thermo analysis (DTA)*

A DTA (Bahr thermo analyse DTA 701) device was used to analyse the thermal properties of the glass-ceramics (ingot and after hot-pressing). The specimens were ground in an agate

Table 1 – Materials used in this study.

Glass-ceramic materials	LOT No	Manufacturer	Investment material	LOT No	Press furnace
IPS e.max Press MT A2 (control group)	W13590	Ivoclar Vivadent	IPS PressVest Premium	WL1857	Ivoclar 3010
Initial LiSI Press MT A2	1708041	GC	LiSi PressVest	1802061	Dekema 654i
Celtra Press MT A2	18025681	Dentsply	Celtra Press	7108	Ivoclar 3010

Table 2 – Firing schedule of the heat treatment stimulations.

Stage	Pre-heating temp (°C)	Drying time (min)	Heating rate (°C/min)	Vacuum	Firing temp. (°C)	Dwelling time (min)
Wash firing	430	4	45	+	760	1
1st Dentin firing	430	6	45	+	760	1
2nd Dentin firing	430	6	45	+	750	1
Glaze firing	450	4	45	–	760	1

mortar and the powders heated from room temperature to 1050 °C with a heating rate of 10 °C/min.

2.3. Dilatometry

The thermal expansion coefficients of the glass-ceramics were determined with a dilatometer (Netzsch TMA 402) in the range 20 °C–610 °C with a heating rate of 5 °C/min. The cylinder-shaped specimens (2 of each glass-ceramic) were prepared according to DIN EN ISO 6872:2015 (d = 5 mm, l = 28 mm).

2.4. Opacity and colour

The colour coordinates (CIE L^* a^* b^*) and opacity of the glass-ceramics were investigated with a Konica Minolita device (CM 3610d). The light beam of a xenon flash lamp having a wavelength range of 360 nm to 740 nm and a distance of 10 nm after being divided into reference beam and sample beam passes through the specimens' chamber to the detector. The specimen beam is at an incident angle of 0° and the reference beam at 8°. For detecting the light, a photomultiplier sensitive to the ultraviolet/visible is used to. A black and white background was used to perform the measurements.

L^* is a measure of the lightness-darkness of material (perfect black has an $L^* = 0$, and perfect white has an $L^* = 100$) [38]. The a^* coordinate is a measure of the redness (positive value) or the greenness (negative value), while the b^* coordinate is a measure of the yellowness (positive value), or the blueness (negative value)

[38,39]. 10 specimens of each glass-ceramic were prepared (d = 16 mm, h = 1 mm). The measurements were performed before and after heat treatments.

2.5. Phase identification

2.5.1. Room temperature X-ray diffraction analysis (RT-XRD)

The mineralogy of the specimens was studied by X-ray diffraction technique (Bruker, AXS D8 Advance) using monochromatic Cu $K\alpha 1$ X-rays ($\lambda = 1.5406$ Å). X-ray diffractograms were acquired from 10° to 60° (2θ) with a step size of 0.006° (2θ) and a counting time of 2 s/step. Phase identification was based on ICSD reference data.

2.5.2. High temperature X-ray diffraction analysis (HT-XRD)

The high temperature X-ray measurements were performed on a Rigaku Smartlab 9 kW with a HyPix-3000 2D detector in 1D mode, utilizing an Anton-Paar DHS 1100 heating stage in an atmosphere of air and at normal pressure. Measurements were conducted in intervals of 20 °C while heating as well as during cooling after reaching the maximum temperature. The step size was chosen to be 0.02° for the $\theta/2\theta$ range between 10°–60° at a scanning speed of 10 °/min.

The high temperature X-ray investigation was performed on ingot specimens.

2.6. Raman spectroscopy

A micro-Raman spectrometer (DILOR Labram II, equipped with an Olympus microscope, with an external diode-pumped solid-state laser) was used to further investigate the solid phase mineralogy and extent of crystallization of the glass-ceramics. Data were acquired at 532 nm exciting wavelength in confocal mode in the range of 100–1400 cm^{-1} wave numbers. The spectral and spatial resolution was 2 cm^{-1} and <2 μm, respectively [43]. 10 measurements were performed for each sample.

2.7. Scanning electron microscopy (SEM)

The microstructure analyses were performed using a Field Emission Scanning Electron Microscopy (FESEM, Carl Zeiss Ultra, Oberkochen, Germany). The polished specimens were used to study the microstructure of the glass-ceramics. The investigation of the crystallite microstructure was performed on polished and etched specimens. The etching was performed for 5 min with a 5% hydrofluoric acid gel (Vita Zahnfabrik, Germany), thereafter the specimens were washed with distilled water. The acceleration voltage and working distance was 5 kV and 8 mm, respectively. All specimens were gold sputter-coated before SEM analysis for preventing charging effects during imaging.

2.8. Roughness

The roughness of the polished specimens was investigated with a confocal 3D Laser Scanning Microscope (Keyence), equipped with a red laser (658 nm wavelength, semiconduc-

tor). The magnifications, operation distance and numerical aperture (NA) were 50×, 0.54 mm and 0.8, respectively. The size of detector was 1024 × 768 pixels. The pixel resolution was 0.2 μm. The specimens were mounted on a XY cross table. The calculation of the roughness was performed with Analyse-Modul software (Keyence, Japan).

Ra is the average of absolute value (μm) along the reference length and the

Rt is the vertical distance between the highest peak and the deepest valley along the evaluation length

Rz is the absolute vertical distance (μm) between the highest peak and deepest valley along the reference length (see Hallmann) [40].

2.9. Biaxial flexural strength

Biaxial flexural strength was measured according to DIN EN ISO 6872:2015. To study the effect of the heat and etching treatments on this important physical property, 30 specimens of each glass-ceramic were prepared. The diameter (d) and thickness (h) of the specimens were as follows: $d = 14 \pm 2$ mm and $h = 1.2 \pm 0.2$ mm (DIN ES ISO: 6872:2015). The disc specimens were centred and supported on three steel spheres ($d = 2.5$ mm) located on a circle ($d = 10.1$ mm) separated by equal distances. The specimens were loaded in a universal testing machine (Zwick Z 010, Ulm, Germany) with a 50 N load cell at a crosshead speed of 0.5 mm/min and run until failure. The flexural strength was calculated as follows:

$$\sigma = -0.2387P(X\text{-}Y)/b^2$$

σ is the flexural strength (MPa), P is the total load required for fracture (N),

$$X = (1+\nu)\ln(r_2/r_3)^2 + [(1-\nu)/2](r_2/r_3)^2$$

$$Y = (1+\sigma)[1 + \ln(r_1/r_3)^2] + (1-\nu)(r_1/r_3)^2$$

ν is Poisonś ratio

r_1 is the radius of the support circle (mm), r_2 is the radius of the loaded area (mm)

r_3 is the radius of the specimen (mm), and

b is the thickness of the specimen (mm).

2.10. Vickers hardness

A Vickers Hardness tester (Model 3213, Ulm Germany) with a load of 19.62 N and a dwell time of 10 s was utilized to determine the surface hardness of three glass-ceramics. The two indent diagonals were measured immediately after the load was released. The average value of the indent diagonals was used to calculate the Vickers hardness (H, GPa) according to ASTM C 1327-08. Five specimens of each glass-ceramic were prepared for these measurements. Five indentations were measured for each specimen, and the average value was calculated. Vickers hardness was measured on the polished surface of the ingot and of the hot-pressed specimens. The measurements were also carried out on the specimens' surface after heat treatments.

2.11. Fracture toughness

The fracture toughness was measured using the indentation technique. For this, a Vickers hardness indenter was used. The calculation of the fracture toughness (K_{IC}) was performed as follows:

$K_{IC} = 0.016\,(E/H)^{1/2}(P/c)^{3/2}$ where H is the Vickers hardness, E the elastic modulus, P the indentation load applied and c the crack length measured from the centre of the indent [41].

2.12. Chemical composition of specimens

The composition of the glass-ceramics where semi-quantitatively determined, employing a combination of standardized SEM-EDS analyses and Laser-ablation ICP-MS (LA-ICP-MS) analyses. Ingots were embedded in epoxy resin, ground to expose a horizontal cross section and polished to 1 μm diamond suspension. Samples were coated with 20 nm of carbon and analysed for major and minor elements with a scanning electron microscope (JEOL JSM-6390LA) equipped with a Thermo Fisher NSS7 EDS system with a 30 mm^2 silicon drift detector. We conducted standardized analyses employing a series of oxide and silicate standards and the Phi-Rho-Z matrix correction procedure considering Li_2O as difference element to 100 wt.%. For each specimen 12–21 individual analyses with a spot-size of about 15 × 15 to 25 × 25 μm were acquired and averaged. Standards were only available for Si, Al, Mg, Fe, Ca, Na, K and Ti, all other elements where characterized with a standard-less method (P, Zr, Hf, REE, Zn, V, B).

In a second step the samples were analysed by LA-ICP-MS to quantify Li that cannot be analysed by characteristic X-ray methods. The instrument is composed of 193 nm ArF Excimer laser coupled with an Elan 6100 DRC from Perkin Elmer. Standard reference material is NIST SRM 610. For each sample three spots with a diameter of 90 μm were analysed. The program SILLS was used to reduce the obtained data (Guillong et al., 2008) [42]. SiO_2 (wt.%) concentrations previously determined by standardized SEM-EDS analyses were employed for absolute quantification; elements were recalculated to oxide (wt.%). The combination of SEM-EDS and LA-ICP-MS allowed unequivocal identification of elements with concentrations > 0.1 wt.% and the determination of absolute concentrations with an uncertainty of about 10% relative.

3. Results

3.1. Differential thermo analysis (DTA)

As evident from Fig. 1 and Table 3 IPS e.max Press and initial LiSi Press specimen did not reveal any crystallization temperature. The melting temperature for these materials was 955 °C. A transformation peak in the range 338 °C–342 °C was observed for all glass-ceramics and is attributed to SiO_2 impurities. The DTA plots of Celtra Press ingot and hot-pressed specimens were identical and resulted the same three peaks (Fig. 1, Table 3). The peak intensity at 833 °C–847 °C was highest and attributed to the crystallization temperature of the LS2 phase (Fig. 1, Table 3).

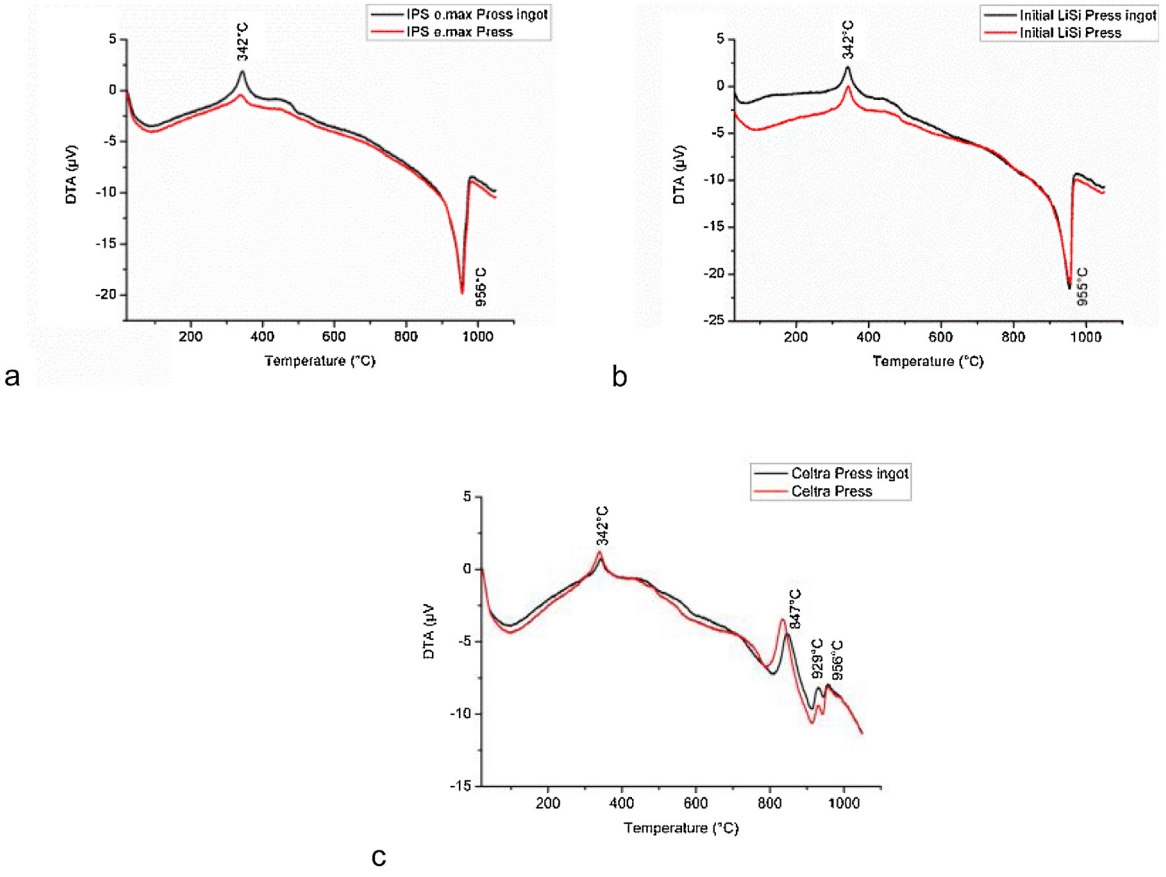

Fig. 1 – DTA plots of ingot and hot-pressed specimens: (a) IPS e.max Press, (b) Initial LiSi Press, (c) Celtra Press.

Table 3 – Thermal data of three LS2 glass-ceramics.

Specimens	T (°C)	T_c (°C)	T_m (°C)
IPS e.max Press (ingot)	343	–	955
IPS e.max Press	338	–	956
Initial LiSi Press (ingot)	342	–	955
Initial LiSi Press	344	–	955
Celtra Press (ingot)	342	845 926 956	913 946
Celtra Press	339	833 930 956	914 941

T_c crystallization temperature.
T_m melting temperature.

3.2. *Dilatometry*

The transition temperatures of LS2 glass-ceramics were increased after heat treatments (Table 4). The values of thermal expansion coefficients (CTE), measured in the range of 20 °C–500 °C, hardly changed after the heart treatments, they only slightly increased when the measurements were performed in the range of 20 °C–600 °C.

The high concentration of ZrO_2 (about 9 wt.%, Table 6) in the Celtra Press specimens increased T_g. Initial LiSi Press glass-ceramic was characterized by a lower α-value compared to the other glass-ceramics (Table 4).

3.3. *Effect of heat treatment on the opacity and colour*

A high opacity was observed for IPS e.max Press specimens. After heat treatments the opacity hardly changed. An increase in opacity after heat treatments was observed for initial LiSi Press and Celtra Press specimens (Fig. 2). The opacity of Ini-

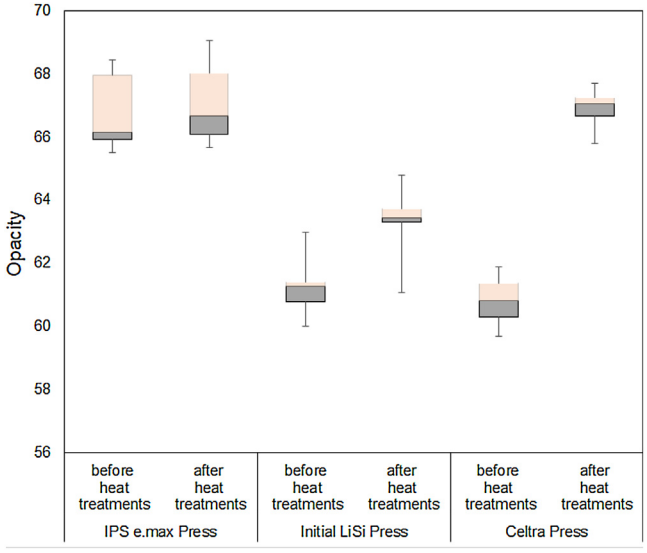

Fig. 2 – Effect of the heat treatments on the opacity of three LS2 glass-ceramics.

Table 4 – Thermal expansion coefficients and transition temperature of three LS2 glass-ceramics.

Specimens	$\alpha_{20\text{-}500^\circ C}$ (10^{-6} K^{-1}) before heat treatments	$\alpha_{20\text{-}600^\circ C}$ (10^{-6} K^{-1}) before heat treatments	$\alpha_{20\text{-}500^\circ C}$ (10^{-6} K^{-1}) after heat treatments	$\alpha_{20\text{-}600^\circ C}$ (10^{-6} K^{-1}) after heat treatments	T_g (°C) before heat treatments	T_g (°C) after heat treatments
IPS e.max Press	10.41	10.99	10.29	11.22	502	520
Initial LiSi Press	9.55	9.67	9.66	10.34	522	556
Celtra Press	9.77	10.45	9.69	11.00	538	548

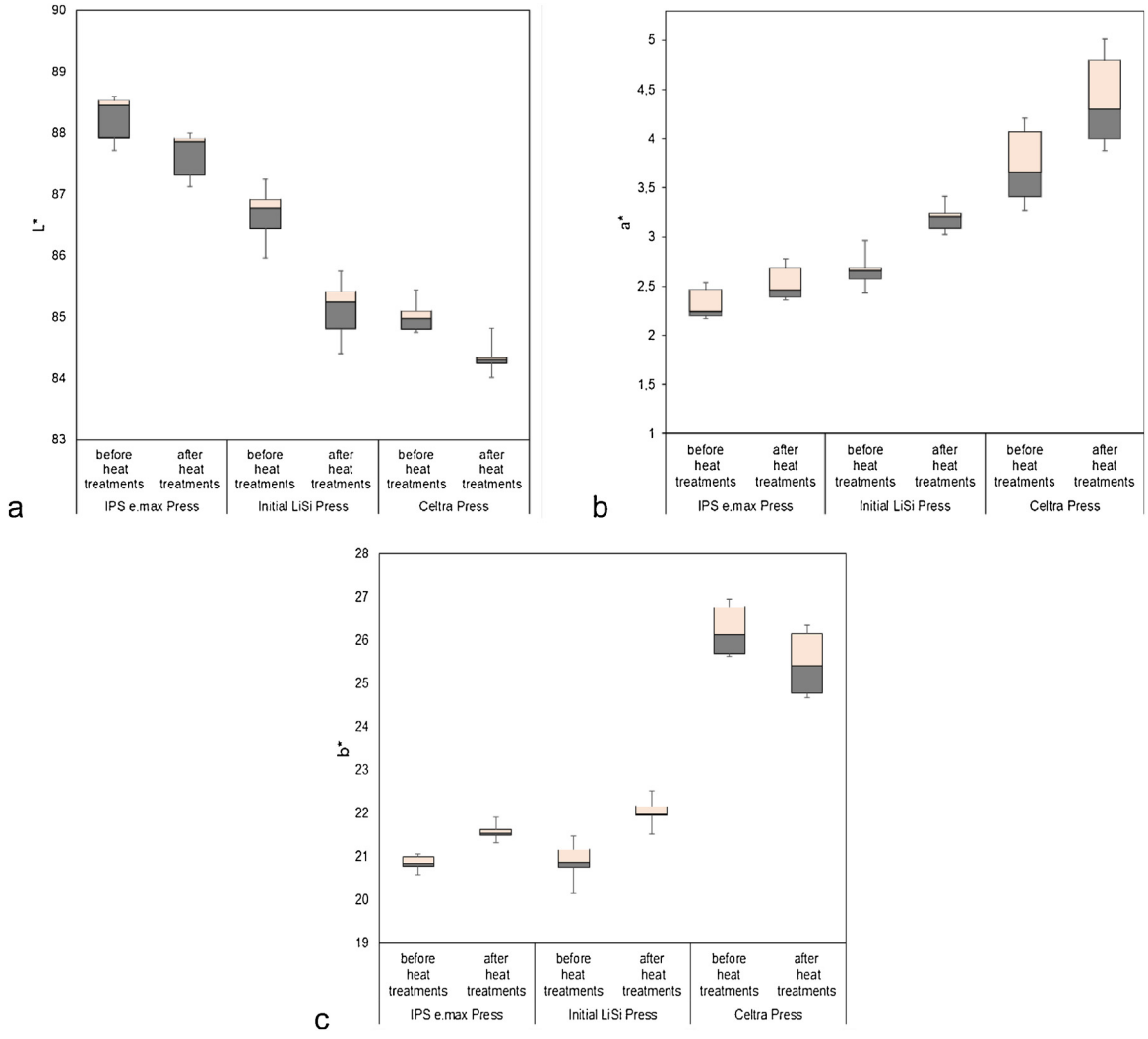

Fig. 3 – Effect of the heat treatments on the colour of three LS2 glass-ceramics.

tial LiSi Press was between the opacity of IPS e.max Press and Celtra Press specimens.

According to manufacturers' data, the glass-ceramics used in this study have the same translucency (medium, MT) and colour (A2). As evidenced in Fig. 3, high values in L^* were observed for the IPS e.max Press (before heat treatments) followed by the initial LiSi Press specimens while low values were observed for Celtra Press specimens (Fig. 3). After heat treatments, a slight reduction in L^* values were observed for all LS2 glass-ceramics (Table 5). After heat treatments, the a^* values were increased for all LS2 glass-ceramics, corresponding to an increase in the red colour. The increase in the b^* values for IPS e.max Press and Initial LiSi Press specimens (Table 5) resulted in an increase in the yellow colour, while the reduction in b^* values for Celtra Press resulted in an increase in blue colour related to heat treatments.

Table 5 – Average change values of L* a* b* after heat treatments.

Specimens	ΔL^*	Δa^*	Δb^*
IPS e.max Press	−0.605 (±0.049)	0.210 (±0.032)	0.739 (±0.100)
Initial LiSi Press	−1.568 (±0.120)	0.523 (±0.049)	1.135 (±0.141)
Celtra Press	−0.657 (±0.089)	0.648 (±0.102)	−0.741 (±0.196)

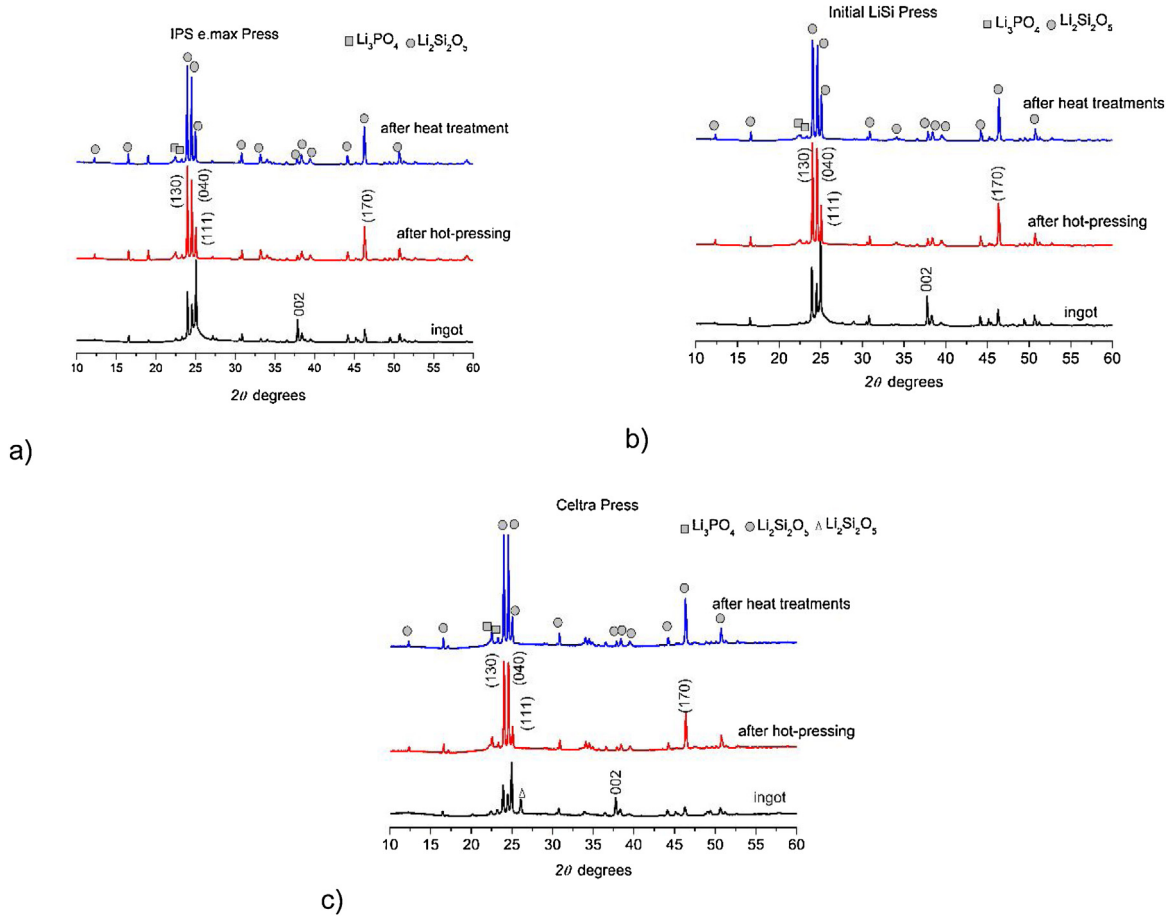

Fig. 4 – RT-X-ray pattern of IPS e.max (a), Initial LiSi Press (b) and Celtra Press (c) specimens: ingot, after hot-pressing and after heat treatments.

3.4. *Room temperature XRD*

The main phase of all glass-ceramics before hot-pressing was $Li_2Si_2O_5$ (LS2) with the highest intensity for the (111) reflex. As a minor phase lithium orthophosphate (see Fig. 4) was identified. A peak with high intensity was detected at $2\theta = 26.107°$ for Celtra Press specimens (ingot) which corresponded to the lithium metasilicate phase Li_2SiO_3. No peak associated with a zirconia phase was detected for this material. Lower intensities of the main peaks of the LS2 phase were observed for the Celtra Press ingot specimens (Fig. 4). After the hot-pressing process, the intensities of these main peaks changed for all glass-ceramics (Fig. 4). A decrease in the intensity of the (111) and (002) reflections was observed while the intensity increased for the (040) and (170) reflections (Fig. 4). A reduction in background intensity was observed for all glass-ceramics (Fig. 4), with a higher reduction for Celtra Press specimens. After the hot-pressing process, the peaks of some minor phases vanished. The peak at $2\theta = 26.107°$ of the ingot specimens (Celtra Press) was disappeared.

3.5. *High-temperature - XRD*

Fig. 5 reveals that Initial LiSi Press glass-ceramic is stable at high temperature. For this material, no significant change in the intensity ratio of the main peaks was observed over the entire temperature ranges studied. For the IPS e.max Press glass-ceramic, a significant increase in the peak intensities in the range of $2\theta = 28°–37°$ was observed for temperatures more than 900 °C. The LS2 phase was not completely dissolved in the glass matrix at these temperatures, but an intensity ratio change was clearly observed for the three main peaks of this phase. After the cooling process, the crystalline structure was different from that before heating. At temperatures above 880 °C, the LS2 phase in Celtra Press ingot specimens disappeared. For this material, an increase in the intensity of the peaks in the range of $2\theta = 30°–37°$ was observed. During the cooling process, very minor crystallization of the LS2 phase occurred (Fig.5).

3.6. *Raman Spectroscopy*

Fig. 6 illustrates that the intensity of the Raman vibration modes of the IPS e.max Press and the Initial LiSi Press specimens are very similar, which can be explained by the high crystallinity of these materials. A significantly lower intensity of Raman modes was observed for Celtra Press ingot specimens. After the hot-pressing and heat treatments, no significant intensity increase was observed for Celtra Press specimens.

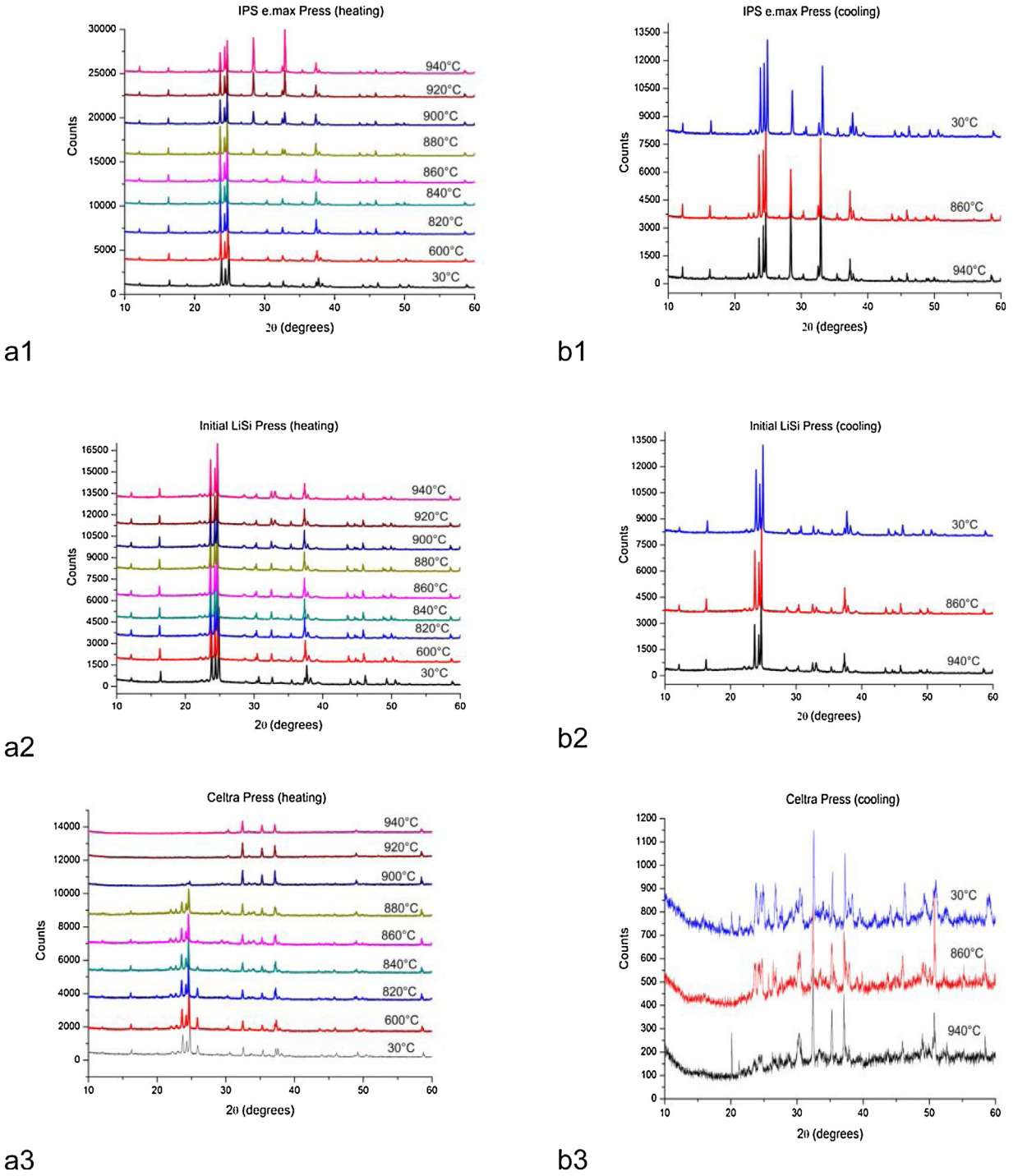

Fig. 5 – High-temperature- X-ray pattern of the ingot specimens. Heating cycles: a1 IPS e.max, a2 Initial LiSi Press, a3 Celtra Press. Cooling cycles: b1 IPS e.max, b2 Initial LiSi Press, b3 Celtra Press.

3.7. *Microstructure*

Fig. 7 shows the microstructures of the glass-ceramics: ingots, after hot-pressing and after additional heat treatments. The IPS e.max ingot specimens exhibit typically rod-shaped crystals. The crystals have an average length of 1.4 μm and an average aspect ratio of about 3.1 forming an interlocking microstructure (Fig. 7A1, B1). After pressing, the crystals aligned parallel to the pressing direction and the specimens' surface (Fig. 7A2, B2). The average length of the crystals increased to 2.7 μm with an aspect ratio of about 5.1. During the heat treatments, the length of the crystals further increased to 3.0 μm with an aspect ratio of about 5.6. The crystals formed again an interlocking arrangement (Fig. 7A3, B3).

The microstructure of Initial LiSi press ingot specimens is quite different compared to the IPS e.max Press ingot specimens. Multi-layered platelet-shaped crystals embedded in

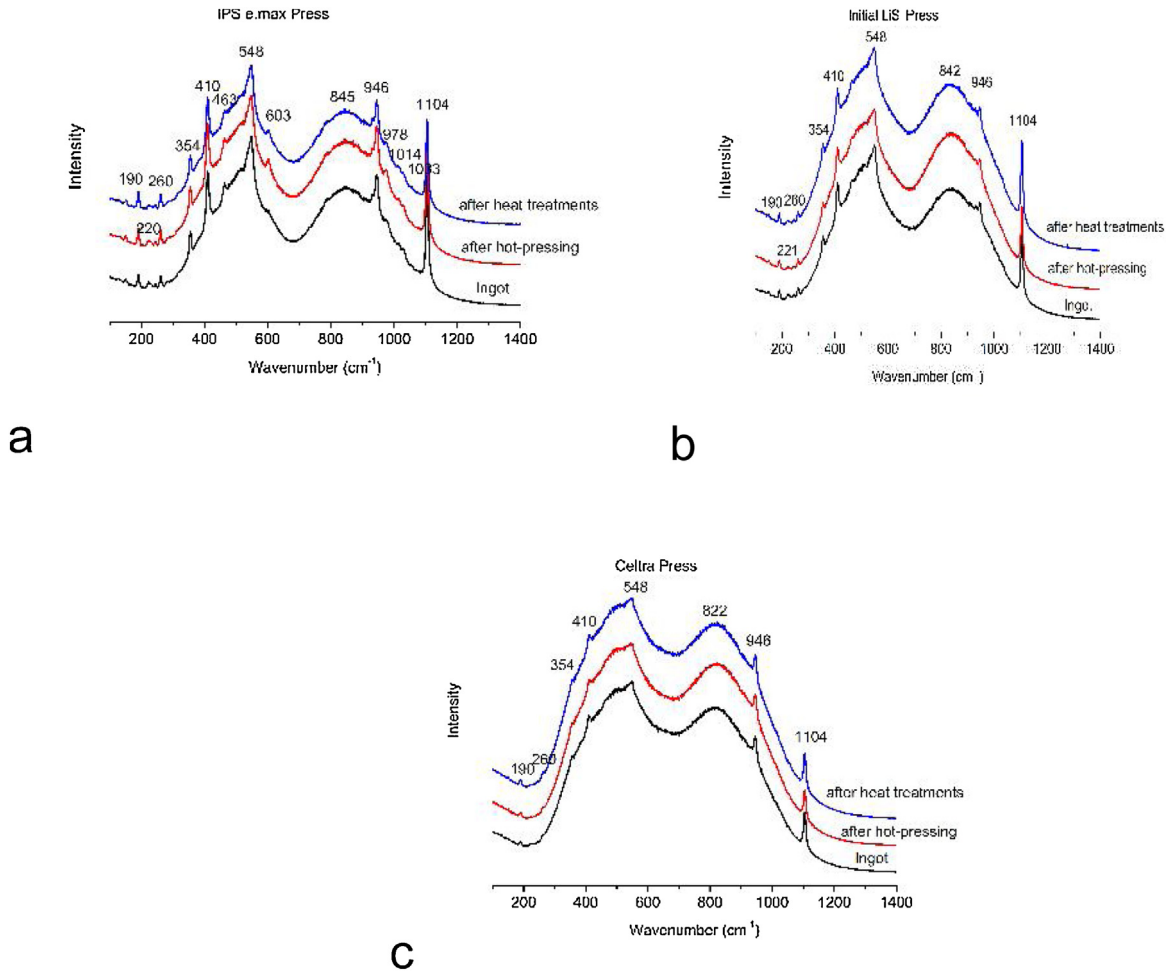

Fig. 6 – Room-temperature Raman spectra of IPS e.max Press (a) Initial LiSi Press (b) and Celtra Press specimens (c) ingot, after hot-pressing and after heat treatments.

the residual glass matrix formed an interlocking microstructure. The average length of the crystals was about 1.4 μm and the aspect ratio of about 4.3 (Fig. 7A4, B4). The average length of the crystals after pressing increased to around 2.1 μm with an aspect ratio of about 4.1. Compared to the IPS e.max Press specimens, the crystals were not aligned parallel to the pressing direction (Fig. 7A5, B5). The heat treatments hardly affected the crystal size and its morphology. The average length was about 2.2 μm with an aspect ratio of about 4.0 (Fig. 7A6, B6). Another microstructure was observed for the Celtra Press ingot specimens. Lath-like crystals of regular and irregular shapes, are randomly aligned and embedded in the glass matrix. The crystal length was about 0.5 μm with an aspect ratio of about 1.3 (Fig. 7A7, B7), (Fig. 8).

After hot-pressing, the crystals size showed a large increase along one axis (Fig. 7A8, B8). The length changed from around 0.5 μm (ingot specimens) to around 1.8 μm (hot-pressed specimens) with an aspect ratio of about 4.6. The crystals changed their morphology into a monolithic belt-like shape, and formed an interlocking microstructure (Fig. 7A8, B8). The crystallisation continued during the heat treatments. The length of the crystals increased further to approximately 2.2 μm with an aspect ratio of about 4.4 (Fig. 7A9, B9).

3.8. *Chemical composition*

The SiO_2 content of the Celtra Press specimens was lower compared to the other glass-ceramics. The content of Al_2O_3 was highest for the Initial LiSi Press specimens (5.4 wt.%) compared to the other glass-ceramics. The IPS e.max Press specimens exhibited a high content of K_2O (4.5 wt.%). A high content of P_2O_5 (4.9 wt.%) was found in the Cetra Press specimens followed by IPS e.max Press specimens (3.7 wt.%). The Celtra Press specimens differed from the other glass-ceramics in their high content of ZrO_2 (9.3 wt.%) and Tb_2O_3 (3.3%) (Table 6).

3.9. *Biaxial flexural strength*

The biaxial flexural strengths of the three LS2 glass-ceramics are given in Table 7 and illustrated in Fig. 9. The Initial LiSi Press specimens demonstrated a high average flexural strength of about 520 ± 100 MPa. The average flexural strength of the IPS e.max Press specimens was 446 ± 81 MPa and 458 ± 113 MPa for the Celtra Press. The heat treatments resulted in an increase of the flexural strength for the IPS e.max Press specimens (515 ± 74 MPa) and a degrease for Initial

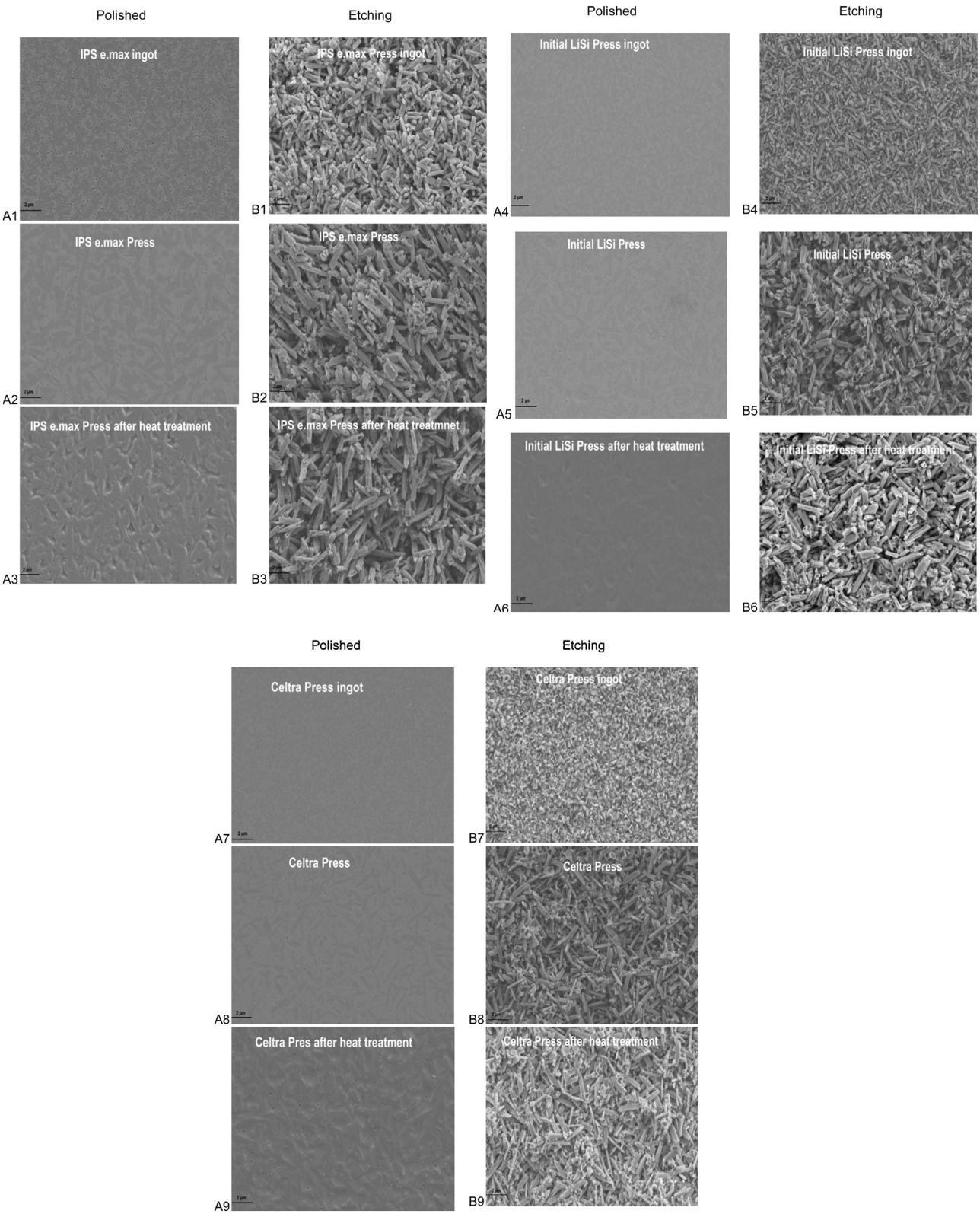

Fig. 7 – SEM images of specimens before and after etching. IPS e.max Press: A1, B1 polished and etched ingot specimens; A2, B2 polished and etched hot-pressed specimens; A3, B3 polished and etched specimens after heat treatments. Initial LiSi Press: A4, B4 polished and etched ingot specimens; A5, B5 polished and etched hot-pressed specimens; A6, B6 polished and etched specimens after heat treatments. Celtra Press: A7, B7 polished and etched ingot specimens; A8, B8 polished and etched hot-pressed specimens; A9, B9 polished and etched specimens after heat treatments.

Table 6 – The chemical composition of the ingot specimens normalized to 100 wt. % oxides.

Oxide	IPS e.mas Press	Initial LiSi Press	Celtra Press
SiO_2	69.2	71.9	59.3
Al_2O_3	2.4	5.4	3.0
Li_2O	14.3	13.0	14.5
K_2O	4.5	2.0	1.2
Na_2O	–	1.4	0.2
P_2O_5	3.7	2.6	4.9
B_2O_3	0.013	0.007	2.0
MgO	0.58	–	0.01
ZnO	1.2	b.d.l.	b.d.l.
ZrO_2	0.67	1.7	9.3
SrO	0.58	–	0,0003
CeO_2	1.8	1.2	0.83
V_2O_5	0.11	0.15	0.61
Tb_2O_3	0.0002	0.35	3.3
Er_2O_3	0.22	0.40	0.73
HfO_2	0.012	0.030	0.21

LiSi Press (502 ± 50 Mpa) specimens. The Celtra Press specimens also showed a slight increase in the flexural strength, 474 ± 113 MPa, but a highly inhomogeneous distribution. The etching process negatively affected the mechanical properties of the LS2 glass-ceramics in this study (Table 7).

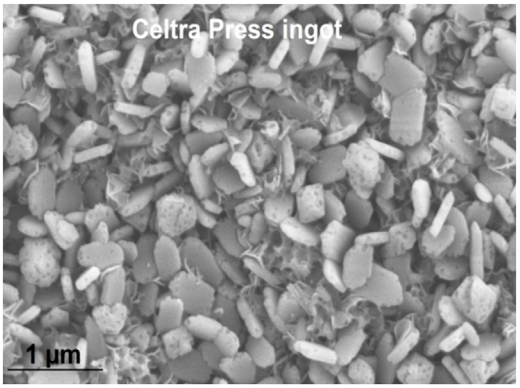

Fig. 8 – SEM image of Celtra Press ingot specimens.

3.10. *Vickers hardness*

The Vickers hardness of the glass-ceramics reveals a decreasing trend for the hot-pressed samples compared to the ingots. A high average hardness was observed for the Initial LiSi Press ingot specimens, 6.7 ± 0.14 GPa. The heat treatments hardly affected the surface hardness (Table 7, Figs. 10 and 11). After the heat treatments, the Initial LiSi Press specimens showed

Table 7 – Mechanical properties of three LS2 glass-ceramics (average values).

Average flexural strength (MPa)								
IPS e.max Press			Initial LiSi Press			Celtra Press		
before heat treatments	after heat treatments	after etching	before heat treatments	after heat treatments	after etching	before heat treatments	after heat treatments	after etching
446 (±81)	515 (±74)	438 (±22)	520 (±100)	502 (±54)	441 (±20)	458 (±113)	474 (±113)	375 (±82)
H20/10 Vickers Hardness (GPa)								
IPS e.max Press			Intial LiSi Press			Celtra Press		
ingot	before heat treatments	after heat treatments	ingot	before heat treatments	after heat treatments	ingot	before heat treatments	after heat treatments
6.3 (±0.16)	6.1 (±0.12)	6.1 (±0.04)	6.7 (±0.14)	6.4 (±0.03)	6.4 (±0.14)	6.6 (±0.05)	6.1 (±0.05)	6.1 (±0.09)
Fracture toughness ($MPa.m^{1/2}$)								
1.03 (±0.06)	0.91 (±0.05)	1.02 (±0.05)	1.02 (±0.04)	0.92 (±0.02)	0.91 (±0.0.04)	0.74 (±0.03)	0.79 (±0.0.02)	0.81 (±0.06)

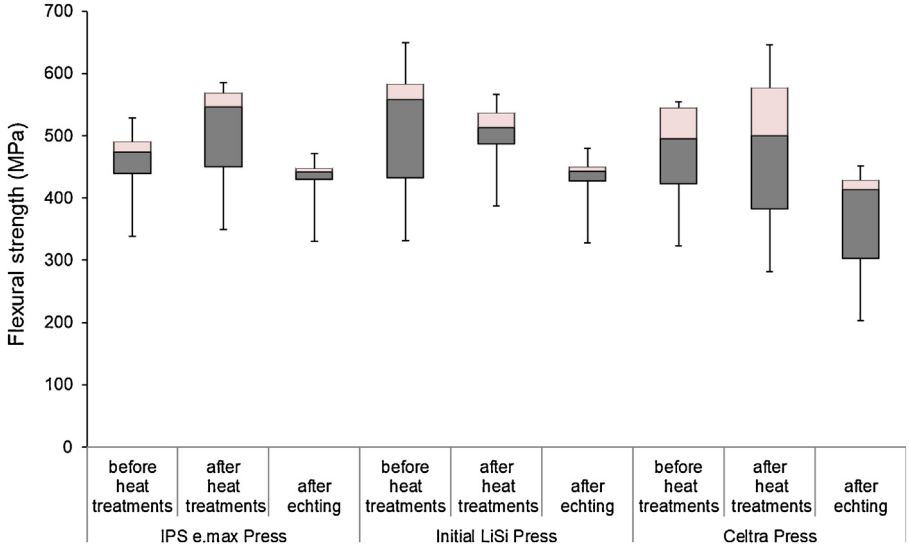

Fig. 9 – Flexural strength of three LS2 glass-ceramics.

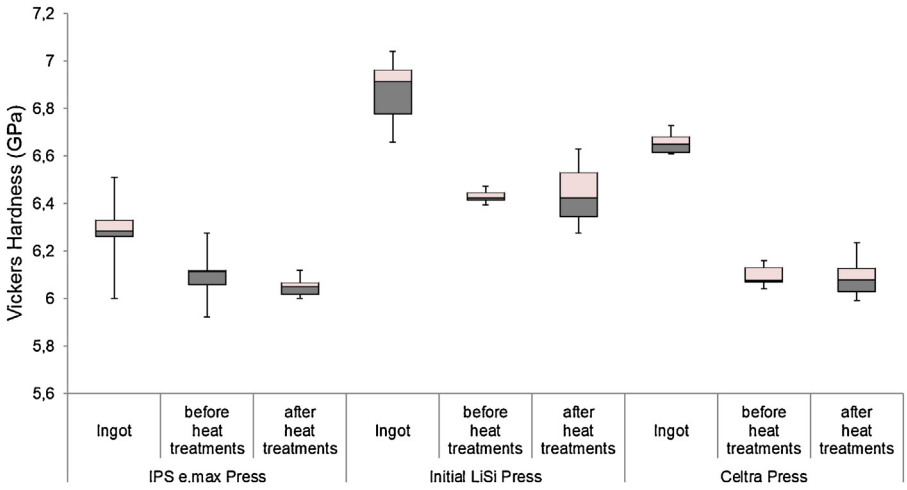

Fig. 10 – Plot of Vickers hardness of three glass-ceramics in this study.

a relatively high value of 6.4 ± 0.14 GPa compared to the other two glass-ceramics (Table 7).

3.11. *Fracture toughness*

The average fracture toughness (K_{IC}) values of the glass-ceramics are summarized in Table 7 and their distribution illustrated in Fig. 12. The IPS e.max Press and Initial LiSi Press ingot specimens were characterized by high K_{IC}, 1.03 ± 0.06 and 1.02 ± 0.05 MPa $m^{1/2}$, respectively (Table 7). A rather low K_{IC} was observed for the Celtra Press ingot specimens with about 0.74 ± 0.03 MPa $m^{1/2}$. After the hot-pressing process, a slight increase in the K_{IC} was observed for the Celtra Press specimens to 0.79 ± 0.02 MPa $m^{1/2}$, while the other two glass ceramics showed a slight decrease (Table 7). The average K_{IC} for the Initial LiSi Press specimens was 0.92 ± 0.02 MPa $m^{1/2}$ and 0.91 ± 0.05 MPa $m^{1/2}$ for the IPS e.max Press. Heat treatment slightly affected the K_{IC}. The IPS e.max Press specimens

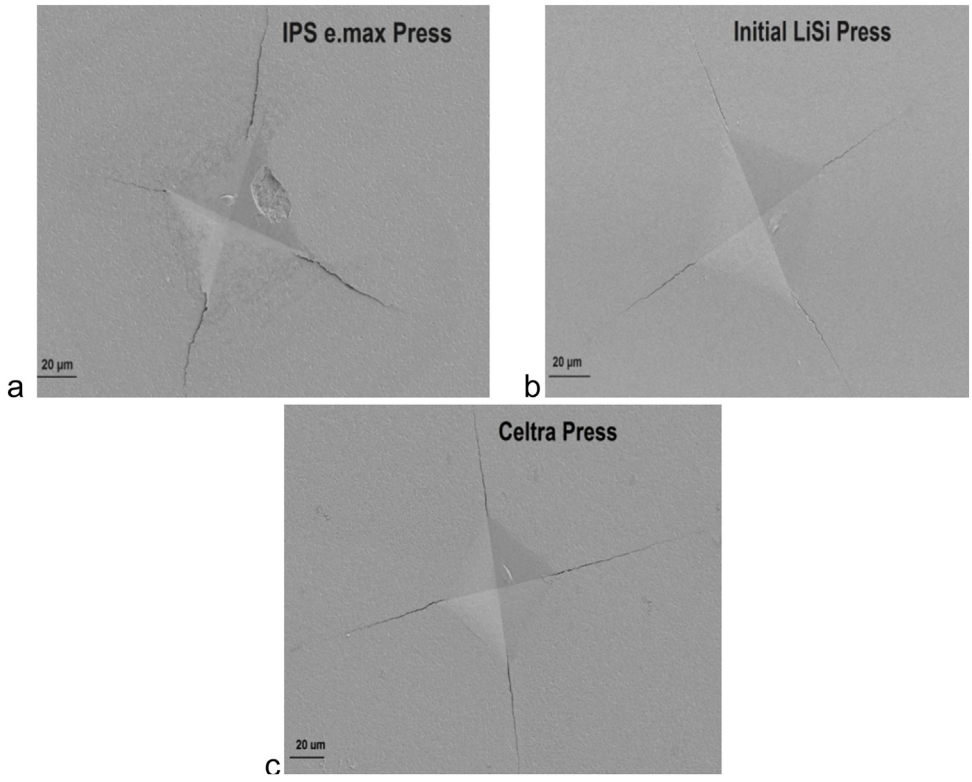

Fig. 11 – SEM images of the Vickers Hardness indentations of IPS e.max Pres (a), Initial LiSi Press (b) and Celtra Press (c) specimens.

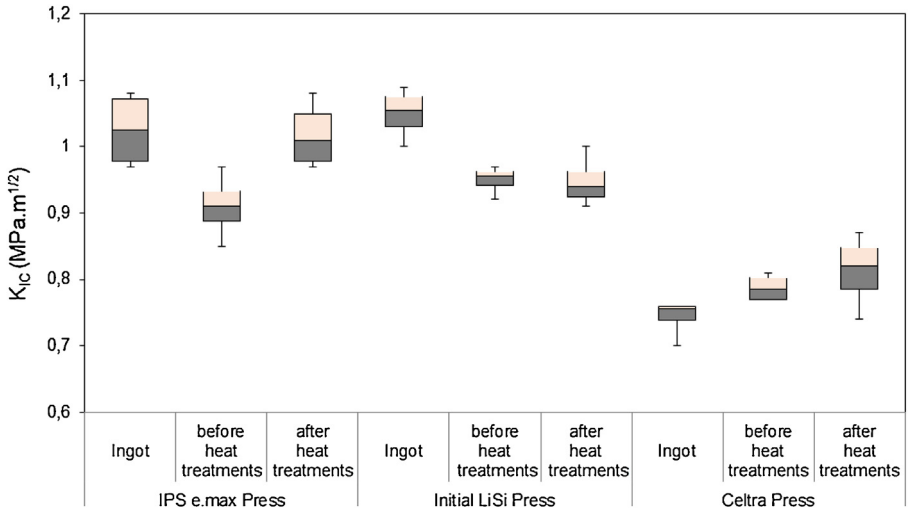

Fig. 12 – Fracture toughness of three glass-ceramics.

Table 8 – Roughness of specimens before and after heat treatments.

Materials	Ra(μm)		Rz(μm)		Rt(μm)	
	before heat treatments	after heat treatments	before heat treatments	after heat treatments	before heat treatments	after heat treatments
IPS e.maPress	0.01 (±0.001)	0.02 (±0.003)	0.05 (±0.002)	0.15 (±0.015)	0.08 (±0.001)	0.21 (±0.011)
Initial LiSi Press	0.01 (±0.001)	0.01 (±0.001)	0.05 (±0.002)	0.06 (±0.007)	0.08 (±0.005)	0.09 (±0.011)
Celtra Press	0.01 (±0.008)	0.03 (±0.001)	0.04 (±0.007)	0.15 (±0.0.003)	0.07 (±0.014)	0.21 (±0.005)

exhibited an increase in the K_{IC} after heat treatments (1.02 ± 0.05 MPa m$^{1/2}$) as well as the Celtra Press (0.81 ± 0.06) MPa m$^{1/2}$) (Table 7).

3.12. *Roughness*

After heat treatments, an increase in the roughness values was observed for the IPS e.max Press and Celtra Press specimens (Table 8). The heat treatments did not affect much the roughness of the Initial LiSi Press specimens (Table 8).

4. Discussion

4.1. *Microstructure and phase characterisation*

It is well known that the mechanical properties of the LS2 glass-ceramics depend on the microstructure of their crystals [34]. The IPS e.max Press and the Initial LiSi Press ingot specimens have a different microstructure. They are characterized by rod-shaped and platelet-shaped crystals with approximately equal length and high aspect ratio forming an interlocking microstructure. The multi-layered arrangement of the LS2 crystals in the Initial LiSi Press specimens is a result of an epitaxial growth on the heterogeneous nuclei formed by added nucleating agents [59]. Celtra Press ingot specimens have lath-like crystals with short length and low aspect ratio. After hot-pressing, the crystals in the IPS e.max Press specimens changed their orientation during extrusion by plastic deformation. The alignment of needle-like crystals parallel to the pressing direction may be a result of the viscous flow, plastic deformation and shear stress [45–51]. The crystal alignment during the heat treatments depends on the crystal shape, the proportion, size and viscosity of the remaining glass phase [46–50]. For LS2 glass-ceramics only needle-like crystals (IPS e.max Press) were aligned parallel to the extrusion direction and the specimens' surface. The platelet-shaped crystals were randomly oriented with an interlocking microstructure after the hot-pressing process (Initial LiSi Press and Celtra Press). The X-ray pattern showed an intensity increase of the (040) and (170) reflexes and an intensity decrease of (111) and (002) reflexes for all LS2 glass-ceramics in this study. This increase cannot only be explained by the orientation of these planes parallel to the crystal surfaces and extrusion direction. The crystals in the Initial LiSi Press and Celtra Press specimens were randomly aligned. Therefore, the intensity changes of these reflections cannot be explained by the alignment of crystals alone. One factor which has affected the intensity of the (040), (170), (111), and (002) reflexes is the growth of crystals in <040> direction and <170> during the extrusion process. This change in crystal growth led to an increase of stress in the field around the crystals, which affects the mechanical properties of LS2 glass-ceramics. The needle-like crystals were aligned with their elongated axis parallel to the pressing direction, but the platelet-like crystals did not. This difference in orientation can be explained with the crystal shape and the difference in temperature extrusion and perhaps with the holding time before hot-pressing. The LS2 crystals in IPS e.max Press specimens after the heat treatments were no longer aligned parallel to the extrusion direction. The increase in crystals size after heat treatments observed for IPS e.max Press specimens can be explained by Ostwald ripening. Larger crystals grow at the

expense of smaller ones [47,51]. The lack of peaks associated with crystallization in the DTA graphs excludes residual glass-phase crystallization. The crystal size increase changed the orientation of the crystals into an interlocking microstructure. It is known that the chemical composition plays an important role on the morphology of LS2 crystals [34]. The effect of chemical composition and the preparation of the LS2 glass-ceramic is very well evident in the Celtra Press specimens. The large change in crystal morphology after pressing was a result of the parameters of the ingot production and the chemical composition of the glass phase. The DTA analysis of pressed specimens showed that the crystallization of the LS2 phase in Celtra Press specimens was not completed. Lithium disilicate was the main phase in IPS e.max Press and Initial LiSi Press ingots; other phases like Li_3PO_4 were minor [61]. The absence of lithium metasilicate in these glass-ceramics implies that the preparation of the ingots has been carried out at a temperature of about 830 °C–860 °C where the transformation of the LS phase to the LS2 phase is completed. The presence of the lithium metasilicate phase in Celtra Press ingots implies that this glass-ceramic was produced at a lower temperature resulting in an incomplete transformation of lithium metasilicate into lithium disilicate. After hot-pressing, the LS phase disappeared. The main phase after hot-pressing was lithium disilicate and lithium orthophosphate formed the minor phase. The intensity ratio of the main peaks changed and was in the agreement with the results of Chung et al., and Albakry et al [52,47]. In the literature the structure of the LS2 phase is controversy discussed. Some authors found that the LS2 phase has a monoclinic structure with an important orthorhombic pseudo-symmetry with $\beta \tilde{}$ 90° [47,53]. Other authors found that the LS2 phase has an orthorhombic structure with the space group Ccc2 [54–56]. A comparison of the ICSD data for both structures revealed no clear answer to the structure of the LS2 phase. The 2θ shift observed for all specimens in this study can be attributed to additives like Al_2O_3, K_2O, Na_2O, MgO, P_2O_5, ZrO_2, and pigments. The ZrO_2 content of the Celtra Press specimens was about 10%. The absence of zirconia reflections in the X-ray pattern as well as in the Raman spectra testifies that zirconium oxide is dissolved in the glass phase and serves as a network modifier. The working temperature of the glass silicate depends on the polymerization of the silica network. A high degree of polymerization requires a higher working temperature of the glass silicates. It is known that modifiers are capable of reducing the working temperature due to modification (reduction) of the polymerization of the silica network. There are discussions about the role of ZrO_2 in glass-ceramics [34]. According to the Zacharianen rules, the 6 coordinated Zr^{+4} cations serve as a network modifier and should therefore increase the depolymerization of the silicate network by introducing additional non-bridging oxygens.

Belli et al. used the Raman modes at 603 cm^{-1} and 946 cm^{-1} to identify the LS phase [57]. According to the results of this study, these modes were observed in the IPS e.max Press and very weakly the 946 cm^{-1} also in the Initial LiSi Press specimens where XRD measurements did not reveal any peaks indicative to the LS phase. Our results possibly indicate that these modes should not be used for the identification of the LS phase because these vibration modes belong LS2 phase.

According to the HT-XRD results, lithium metasilicate in the Celtra Press specimens started to react with the glass matrix at 820 °C and completely disappeared at 880 °C. The intensity of the main peaks of the lithium disilicate phase in the range of 23.5–25.3° (2θ) was very low at 900 °C for Celtra Press ingots specimens. At 920 °C the LS2 phase was entirely dissolved in the glass phase. During the cooling process, a very small increase in the intensity of the LS2 main peaks occurred. According to the XRD results, Celtra Press ingots can be processed up to 860 °C–880 °C. Initial LiSi Press was very stable at high temperature. The LS2 phase for this material was stable up to 940 °C. The intensity ratio hardly changed. During the cooling process, the intensity of the main peaks increased, inferring that additional LS2 phase crystallized from the glass matrix. In the case of IPS e.max Press, the LS2 phase was stable up to 900 °C. Above this temperature, the intensity of the peaks in the range of 27°–34° (2θ) increased strongly, and the intensity ratio of LS2 main peaks changed. During the cooling process, the crystallization of the LS2 phase continued, but the structure of the LS2 phase was not the same as that of the ingots before the extrusion process. According to HT-XRD results, the working temperature of IPS e.max is up to 900 °C.

The roughness increases after the heat treatments observed for IPS e.max Press and Celtra Press is either due to an increased crystal size as a result of Oswalt ripening process or the crystallization of the glass phase.

4.2. *Optical properties*

In restorative dentistry, the optical properties play an importantly role in the patient satisfaction and restorative success. Translucency of dental materials depends on many factors such as the ratio of the crystalline/glass phases and the difference in the refractive index between these phases, the morphology of crystals, grain boundaries, pores, second-phase component, additives, and light scattering from the surface. Usually, high crystallinity is associated with high opacity when the two phases have a very different refractive index. High translucency of lithium disilicate glass-ceramics is attributed to the matching of the refractive index of the crystal phase to that of the glass matrix [62]. A linear well-organized crystalline structure increases the transmittance of these materials. The opacity of IPS e.max Press is attributed to the interlocking microstructure of LS2 crystals and their sizes. The effect of heat treatments on the optical properties (colour and opacity) of IPS e.max Press, Initial LiSi press and Celtra Press could be explained with the increase of the crystal size, the orientation of the crystals and perhaps with the change of the glass matrix.

4.3. *Mechanical properties*

The fracture toughness is a bulk material property, while the strength depends on the surface conditions [58]. The fracture toughness is influenced by the local stress field resulting from a second phase in the crystal/glass phase separation, crystallization, thermal expansion anisotropy, thermal expansion mismatch between two phases, elastic anisotropy or mismatch. The stress field created around a second phase particle in a glass or crystalline matrix can lead to toughening

by either micro-cracking or crack deflection/interaction [58]. K_{IC} is an intrinsic material property which describes the materialś ability to withstand unstable crack propagation and correlates with its clinical performance (fracture and wear) [44,21]. The mechanical failures were always accompanied by a crack-initiation/crack propagation process and the values of K_{IC} are used to predict the clinical performance of the dental ceramics [44] The microstructure of glass-ceramics has a great impact on the fracture toughness of these materials. The fracture toughness generally increases with the volume fraction of the crystalline phase and the size of crystals. It increases with increasing grain size up to a certain limiting value. From this point on it decreases with further increasing grain size due to the existence of micro-cracks [58]. Elongated crystallites increase the fracture toughness more than equigranularity crystallites because longer grains with higher aspect ratio further increase the energy required for crack propagation [47]. The results of this study confirmed the concept that fracture toughness depends on the aspect ratio of the crystals. Celtra Press ingots specimens with low aspect ratio of crystals resulted low fracture toughness. The comparatively high glass content in the Celtra Press ingots favoured the crack propagations until the crack tip encounters the first crystallites and confirmed the idea that the fracture toughness also depends on the volume fraction of the second phase (crystalline phase). The Initial LiSi Press and IPS e.max Press ingots specimens demonstrated a high fracture toughness. The crystals of these glass ceramics have a different morphology, platelet- and rod-like. According to the results of this study, the fracture toughness also depends on the alignment of crystals to the load. The interlocking microstructure and the alignment of rod-like crystals with their longest axes perpendicular to the load increase the fractural strength. In the case of platelet-like crystals, it is important that the alignment of the shortest crystal axis is perpendicular to the beam. An increase in fracture toughness after the hot-pressing process was to be expected due to the crystal grain size increase. This was only observed for Celtra Press specimens because of the large increase in the crystals size. The slight decrease of this parameter for the other LS2 glass-ceramics can be explained with the non-interlocking microstructure and the residual stresses resulting from a temperature gradient during manufacturing, the density changes introduced by the crystallization process, and by the CTE mismatch between glass and crystalline phases [53,54].

Flexural strength usually represents the ability to tolerate chewing force [9]. It is an important factor for the success of any fixed restorations [10,11]. The microstructure plays an important role on the flexural strength of LS2 glass-ceramics. The high flexural strength of 520 MPa of Initial LiSi Press specimens means that not only rod-like crystals can enhance flexural strength of LS2 glass-ceramics, but also platelet-like crystals. The low flexural strength values observed for Celtra press are in agreement with the results of Apel et al. [60] According to these authors, the incorporation of ZrO_2 in the glass matrix does not increase the flexural strength. This can be explained by the increase in viscosity due to the high ZrO_2 content in the glass- ceramic and the associated reduction in the crystal growth of LS and LS2 [60]. In the case of the platelet-shapes crystals, the flexural strength is depended on the orientation of these crystals to the load beam.

The etching process has a negative effect on the flexural strength of LS2 glass-ceramics. The results of this study are in agreement with the results of Hooshmand et al. [12]. According to these authors, the etching process reduced the biaxial flexural strength significantly. The residual compressive stresses generated at the crystal/glass interfaces during the crystallization process were removed with removing the glass phase around the crystals, resulting in a decrease in flexural strength.

5. Conclusions

The mechanical properties of the LS2 glass-ceramics depend on any factors such as the microstructure, the chemical composition, the morphology of the crystals, the properties of the residual glass matrix, the phase composition, the volume ratio crystal/glass. The interlocking microstructure improves the mechanical properties of the glass-ceramics. The increase of the crystal content improves the flexural strength and fracture toughness. The alignment of LS2 crystals along the extrusion direction and parallel to the surface depends on the shape of the crystals was observed only for rod-shaped crystals. The physical properties of platelet-shaped crystals depend on their spatial orientation. Heat treatments, which is a routine process in the restorative dentistry, affected the mechanical and optical properties of LS2 glass-ceramics. Etching with etched gel had a negative effect on the flexural strength. HT-XRD analysis reveals that maximum processing temperatures amount up to 900 °C for IPS e.max Press, to 940 °C for initial LiSi Press, and to 860–880 °C for Celtra Press. The melting temperature was about 960 °C or LS2 glass-ceramics in this study. The absence of ZrO_2 and/or $ZrSiO_4$ reflections in the X-ray diffractograms and in the Raman spectra for the Celtra Press specimens indicates that ZrO_2 is dissolved in the glass matrix and serves as a network modifier.

REFERENCES

[1] Kern M, Thompson VP, Frankerberger R, Kohal RJ, Kunzelmann KH, Pospiech P, et al. All-ceramics at a glance. Soc Dent Ceram 2016:6–14.

[2] Rekow ED, Silva NRFA, Coelho PG, Zhang Y, Guess P, Thompson VP. Critical review in oral biology and medicine. J Dent Res 2011;90:937–52.

[3] Kelly JR, Benetti P. Ceramic materials in dentistry: historical evolution and current practice. J Aust Dent 2011;56:84–96.

[4] Wang RR, Lu CL, Zhang DS. Influence of cyclic loading on the fracture toughness and load bearing capacities of all-ceramic crowns. Int J Oral Sci 2013;6:99–104.

[5] Zarone F, Ferrari M, Mangano G, Leone R, Sorrentino R. Digitally oriented materials, focus on lithium dislicate ceramics. Int J Dent 2016:1–10.

[6] Peng Z, Rahman MIAR, Zhang Y, Yin L. Wear behaviour of pressable lithium disilicate glass ceramic. J Biomed Mater Res B Appl Biomater 2016;104:968–78.

[7] Yang Y, Yu J, Gao J, Guo J, Zhao Y, Zhang S. Clinical outcomes of different types of tooth-supported bilayer lithium disilicate all-ceramic restorations after functioning up to 5 years: a retrospective study. J Dent 2016;51:56–61.

[8] Huettig F, Gehrke UP. Early complications and performance of 327 heat-pressed lithium dislicate crowns up to five years. J Adv Prosthodont 2016;8:194–200.
[9] Kang SH, Chang J, Son HH. Flexural strength and microstructure of two lithium disilicate glass ceramics for CAD/CAM restoration in the dental clinic. Restor Dent Endod 2013;38:134–40.
[10] Mohsen C. Corrosion effect on the flexural strength & micro-hardness of ips e-max ceramics. Open J Stomatol 2011;1:29–35.
[11] Ban S, Anusavice KJ. Influence of test method on the failure stress of brittle dental materials. J Dent Res 1990;(December):1791–9.
[12] Hooshmand T, Parvizi S, Keshvand A. Effect of surface acid etching on the biaxial flexural strength of two hot-pressed glass ceramics. J Prosthodont 2008;17:415–9.
[13] Quinn JB, Sundar V, Lloyd IK. Influence of microstructure and chemistry on the fracture toughness of dental ceramics. Dent Mater 2003;19:603–11.
[14] Bona AD, Mecholsky Jr JJ, Anusavice KJ. Fracture behaviour of Lithia disilicate- and leucite-based ceramics. Dent Mater 2004;20:956–62.
[15] Fuji T, Nose T. Evaluation of fracture toughness for ceramic materials. IJIS Int 1989;29:717–25.
[16] Quinn GD, Salem J, Cho K, Bar-on I, Foley M, Fang H. Fracture toughness of advanced ceramics at room temperature. J Res Nat Inst Stand Technol 1992;97:579–607.
[17] Serbena FC, Mathias I, Foester CE, Zanotto ED. Crystallization toughening of a model glass-ceramic. Acta Mater 2015;86:216–28.
[18] Kruzic JJ, Kim DK, Koester KJ, Ritchie RO. Indentation techniques for evaluating the fracture toughness of biomaterials and hard tissues. J Mech Behav Biomed Mater 2009;2:384–95.
[19] Chantikul P, Anstis GR, Lawn BR, Marschall DB. A critical evaluation of indentation techniques for measuring fracture toughness: II, strength method. J Am Ceram Soc 1981;64:539–43.
[20] Marschall DB, Noma T, Evans AG. A simple method for determining elastic-modulus-to-hardness ratios using Knoop indentation measurements. J Am Ceram Soc 1982;65:c175–6.
[21] Kelly JR. Dental ceramics: what is the stuff anyway? JADA 2008;139:45–75.
[22] Kelly JR. Dental ceramics: current thinking and trends. Dent Clin N Am 2004;48:513–30.
[23] Höland W, Rheiberger V, Apel E, Ritzberger C, Rothbrust F, Kappert H, et al. Future perspektives of biomaterials for dental restoration. J Eur Ceram Soc 2009;29: 1291–7.
[24] Höland W, Rheinberger V, Apel E, Hoen C, Höland M, Dommann A, et al. Clinical applications of glass-ceramics in dentistry. J Mater Sci Mater Med 2006;17:1037–42.
[25] Denry I, Kelly JR. Emerging ceramic-based materials for dentistry. J Dent Res 2014;93:1235–42.
[26] Zanotto ED. A bright future for the glass-ceramics. Am Ceram Soc Bull 2010;89:19–27.
[27] Mohammed B, Afram B, Nazar Z. An evaluation of the effect of different surface treatment on the hardness and smoothness of pressable ceramic (in vitro study). J Dent Med Sci 2015;14:84–9.
[28] Pollington S. Novel glass-ceramics for dental restorations. J Contemp Dent Pract 2011;12:60–7.
[29] Montazerian M, Zanotto ED. Bioactive and intert glass-ceramics. J Biomed Mater 2017;105:619–39.
[30] Gonzaga CC, Cesar PF, Okada CY, Frederrici C, Neto FB, Yoshimura HN. Mechanical properties and porosity of dental-ceramics hot-pressed at different temperatures. Mater Res 2008;11:301–6.
[31] Gormann CM, McDevitt WE, Hill RG. Comparison of two heat-pressed all-ceramic dental materials. Dent Mater 2000;16:389–95.
[32] Catell MJ, Knowles JC, Clarke RL, Lynch E. The biaxial flexural strength of two pressable ceramic systems. J Dent 1999;27:183–96.
[33] Gonzeli R, Kazazoglu E, Ozkan Y. Flexural properties of leucite and lithium disilicate ceramic materials after repeated firing. J Dent Sci 2014;9:144–50.
[34] Hallmann L, Ulmer P, Kern M. Effect of microstructure on the mechanical properties of lithium silicate glass-ceramics. J Mech Behav Biomed Mater 2018;82:355–70.
[35] Höland W, Schweiger M, Frank M. A comparison of microstructure and properties of the IPS Empress 2 and the IPS Empress glass ceramics. J Biomed Mater Res 2000;53:297–303.
[36] Höland W. Phenomena and mechanisms of crack propagation in glass-ceramics. J Mech Behav Biomed Mater 2008;1:313–25.
[37] Höland W, Beall G. Glass-ceramic and technology 2002:75–84.
[38] Paravina R, Powers J. Esthetic color training in dentistry. St. Louis, Mo: Elsevier Mosby; 2004. p. 51–78.
[39] Kim JB, Paravina R, Chen JW. In Vivo evaluation of color of primary teeth. Peadr Dent 2007;29:383–6.
[40] Hallmann L, Ulmer P, Lehmann F, Wille S, Polonskyi O, Johannes M, et al. Effect of surface modifications on the bond strength of zirconia ceramic with resin cement. Dent Mater 2016;16:631–9.
[41] Anstis GR, Chantikul P, Lawn BR, Marschall DB. A critical evaluation of indentation techniques for measuring fracture toughness: I, direct crack measurements. J Am Ceram Soc 1981;64:533–9.
[42] Guillong M, Meier DL, Allan MM, Heinrich CA, Yardley BWD. Appendix A6: SILLS: a MATLAB-based program for the reduction of laser ablation ICP-MS data of homogeneous materials and inclusions. Mineralogical Assoc Can Short Course 2008;40:328–33.
[43] Hallmann L, Ulmer P, Wille S, Kern M. Effect of differences in coefficient of thermal expansion of veneer and Y-TZP ceramics on the interface transformation. J Prosthet Dent 2014;112:591–9.
[44] Alkadi L, Russe ND. Frakture toughness of two lithium disilicate dental glass ceramics. J Prosthet Dent 2016;116:591–6.
[45] Albakry M, Guazzato M, Swain MV. Biaxial flexural strength and microstructure changes of two recycled pressable glass ceramics. J Prosthdont 2004;13:141–9.
[46] Albakry M, Guanzatto M, Swain MV. Influence of hot pressing on the microstructure and fracture toughness of two pressable dental glass-ceramics. J Biomed Mater Res B Appl Biomater 2004;71:99–107.
[47] Albakry M, Guazzato M, Swain MV. Biaxial flexural strength, elastic moduli, and x-ray diffraction characterization of three pressable all-ceramic materials. J Prosthet Dent 2003;89:374–80.
[48] Habelitz S, Gunter C, Rüssel C. Processing, microstructure and mechanical properties of extruded mica glass-ceramics. J Mater Sci Eng A 2001;307:1–14.
[49] Denry IL, Baranta G, Holloay JA, Gupta PK. Effect of processing variables on the texture development in a mica-based glass-ceramic. J Biomed Mater Res B Appl Biomater 2002;64:70–7.
[50] Guazzato M, Albakry M, Ringer SP, Swain MV. Strength, fracture toughness and microstructure of a selection of all-ceramic materials. Part I. Pressable and alumina glass-infiltrated ceramics. Dent Mater 2004;20:441–8.
[51] Oh SC, Dong JK, Luthy H, Schärer P. Strength and microstructure of IPS e.max Express 2 glass-ceramic after different treatments. Int J Prosthodont 2000;13:468–72.

[52] Chung KH, Liao J-H, Duh J-G, Chan DC-N. The effect of repeated heat-presssing on the properties of pressable glass-ceramics. J Oral Rehabil 2009;36:132–41.
[53] Mastelaro VR, Zanotto ED. Anisotropic residual stresses in partially crystallized Li_2O-$2SiO_2$ glass-ceramics. J Non Cryst Solids 1999;247:79–86.
[54] Pinto H, Ito L, Crovace M, Ferreira EB, Fauth F, Wroblewski T, et al. Surfce and bulk residual stress in $Li_2O.2SiO_2$ glass-ceramics. J Non Cryst Solids 2007;353:2307–17.
[55] Li D, Guo JW, Wang XS, Zhang SF, He L. Effects of crystal size on the mechanical properties of a lithium disilicate glass-ceramic. J Mater Sci Eng A 2016;669:332–9.
[56] Belli R, Wendler M, Ciccone MR, Ligny D, Petschelt A, Werbach K, et al. Fracture anisotropy in texturized lithium disilicate glass-ceramics. J Non Cryst Solids 2018;481:457–69.
[57] Belli R, Wendler M, Ligny D, Cicconi MR, Petschelt A, Peterik H, et al. Chairside CAD/CAM materials. Part 1: measurements of elastic constants and microstructural characterization. Dent Mater 2017;33:84–998.
[58] Mecholsky JJ. Toughening in glass ceramics through microstructural design. In: Brant RC, Evans AG, Hasselman DPH, Lange FF, editors. Fracture Mechanics of Ceramics, 6. 1981. p. 165–80.
[59] Headley TJ, Loehman RE. Crystallization of a glass-ceamic by epitaxial growth. J Am Ceram Soc 1984;67:620–5.
[60] Apel E, Hoen C, Rheinberger V, Hölland W. Influence of ZrO_2 on the crystallization and properties of lithium disilicate glass-ceramics derived from a multi-component system. J Eur Ceram Soc 2007;27:1571–7.
[61] Willard A, Chu TMG. The science and application of IPS e.max dental ceramic. Kaohsiung J Med Sci 2018;34:238–42.
[62] Harianawala HH, Kheur MG, Aple SK, Kale BB, Sethi TS, Kheur SM. Comparative analysis of transmittance for different types of commercially available zirconia and lithium disilicate materials. J Adv Prosthodont 2014;6(6):456–61.